

Design and Performance Checks of the NPL Axial Heat Flow Apparatus

J. Wu · J. Clark · C. Stacey · D. Salmon

Received: 11 October 2013 / Accepted: 24 October 2014 / Published online: 19 November 2014
© Crown Copyright 2014

Abstract This paper describes the design and performance checks of the NPL axial heat flow apparatus developed at the National Physical Laboratory for measurement of thermal conductivity. This apparatus is based on an absolute steady-state technique and is suitable for measuring specimens with thermal conductivities in the range from $10 \text{ W}\cdot\text{m}^{-1}\cdot\text{K}^{-1}$ to $240 \text{ W}\cdot\text{m}^{-1}\cdot\text{K}^{-1}$ and at temperatures between 50°C and 500°C . A uniform heat flow is induced in a cylindrical bar-shaped specimen that is firmly clamped between a guarded heater unit at the top and a water-cooled base. Heat is supplied at a known rate at the top end of the specimen by the heater unit and constrained to flow axially through the specimen by a surrounding edge-guard system, which is closely matched to the temperature gradient within the test specimen. The performance of this apparatus has been checked against existing NPL thermal-conductivity reference materials NPL 2S89 (based on Stainless Steel 310) and BSC Pure Iron (pure iron supplied by the British Steel Corporation with 99.96% purity). The measured data produced by the newly designed NPL axial heat flow apparatus agree with the reference data for NPL 2S89 within 2% and with that of BSC Pure Iron to within 3% at temperatures from 50°C to 500°C . This apparatus is being used to provide accurate measurements to industrial and academic organizations and has also been used to develop a new range of NPL reference materials for checking other experimental techniques and procedures for thermal-conductivity measurements.

Keywords Axial heat flow apparatus · Design · Performance checks · Thermal conductivity

J. Wu (✉) · J. Clark · C. Stacey · D. Salmon
National Physical Laboratory, Hampton Road, Teddington TW11 0LW, UK
e-mail: jiyu.wu@npl.co.uk

1 Introduction

Increasing trends toward the development of advanced engineering materials with properties tailored to meet the ever more stringent requirements in high temperature and safety critical applications, means that accurate thermophysical property data are essential to enable design engineers to select reliably the most suitable alloys, ceramics, and composites. One of the key thermophysical properties in heat management at high temperatures is a material's thermal conductivity. Industrial and academic laboratories normally measure thermal conductivity using either comparative steady-state methods [1–3] or derive it from measurements of heat capacity, density, and transient measurements of thermal diffusivity [4,5]. The United Kingdom's National Physical Laboratory (NPL) and United States' National Institute of Standards and Technology (NIST—formerly the National Bureau of Standards (NBS)) have previously designed their own absolute steady-state facilities with traceability to their respective national standards. This type of absolute steady-state technique is more challenging to design and implement in terms of engineering, heat management, and metrology than transient or comparative techniques. However, steady-state techniques offer the advantage of providing clear and straightforward visibility of the sources and propagation of measurement uncertainties that are essential for providing the traceability required for safety critical applications or for the provision of certified reference materials [6–9].

The NPL Long-Bar apparatus [7] was a UK national standard developed in the early 1980s and although it provided reliable data on metals and alloys, there are still certain elements of its design that allow for improvement. For example, even though the specimen in the Long-Bar apparatus was surrounded by an edge-guard and mounted in a vacuum enclosure, it was heated at the bottom causing strong convection currents within the gap between the vacuum enclosure and the three-zone furnace used to provide the main heating. The lack of coupling between the main source of heat, edge-guard, and the edge of the specimen made it very difficult to obtain a good temperature match between the edge-guard and the edge of the specimen. The NPL Long-Bar apparatus, and also the NPL Short-Bar apparatus which was developed around the same time, both utilized long narrow primary heating elements inserted vertically into the specimen or into a heating block in contact with the specimen. The aspect ratio of the heaters led to a significant temperature drop along their length and resulted in heat loss or gain from the guarding system. An improvement in the heater design was made by NBS in their high-temperature absolute cut-bar apparatus [9] through the use of a flat heater disk, but this arrangement still included heating from the bottom end of the specimen.

However, despite an increasing demand for accurate thermal properties values for materials with high thermal conductivities, neither the NPL Long-Bar and Short-Bar apparatus nor the NBS absolute cut-bar apparatus are still in active service. Therefore, to meet this demand, NPL has developed a new axial heat flow apparatus to improve upon its previous national standard Long-Bar apparatus and the Short-Bar apparatus.

2 Principles and Description of the Axial Heat Flow Technique

The newly designed NPL axial heat flow apparatus is based on an absolute steady-state technique and is designed to measure the thermal conductivity of a material within the range from $10 \text{ W}\cdot\text{m}^{-1}\cdot\text{K}^{-1}$ to $240 \text{ W}\cdot\text{m}^{-1}\cdot\text{K}^{-1}$ at temperatures within the range from 50°C to 500°C . In this apparatus, linear heat flow is induced in a cylindrical bar-shaped specimen by using a guarded heater to apply heat at a known rate at one end and extracting the heat at the other end using an isothermal cooling unit. The heat is constrained to flow axially through the specimen with minimal loss or gain through the use of a linear edge-guard system. The temperatures along the specimen are measured using thermocouples, and the heat flux is determined by the amount of electrical power used to heat the main specimen heater. The electrical power is maintained at a fixed value to obtain an appropriate steady-state temperature gradient along the specimens. Then knowing the specimen's length and cross-sectional area, the thermal conductivity of the specimen can be calculated. This simple calculation given by the following equation is based on Fourier's law:

$$\lambda = \frac{Q/A}{(\Delta T/\Delta x)}, \quad (1)$$

where λ is the thermal conductivity of the test specimen ($\text{W}\cdot\text{m}^{-1}\cdot\text{K}^{-1}$), Q is the power supplied to the specimen heater (W), A is the cross-sectional area of the test specimen (m^2), ΔT is the temperature difference between two thermocouples forming a zone along the test specimen (K), and Δx is the distance between two thermocouples forming a zone along the test specimen (m).

The primary configuration of this apparatus utilizes a specimen with a diameter of 20 mm and a length of 160 mm, which is suitable for materials with a thermal conductivity below $80 \text{ W}\cdot\text{m}^{-1}\cdot\text{K}^{-1}$. This primary configuration has been validated against existing NPL certified reference materials for thermal conductivity NPL 2S89 (Stainless Steel 310) [6] and BSC Pure Iron [8]. When used to measure materials with thermal conductivities higher than $80 \text{ W}\cdot\text{m}^{-1}\cdot\text{K}^{-1}$, alternative configurations are used with specimens having reduced diameters (less than 20 mm) to create higher thermal resistance. This alternative operation has been tested on pure zinc (99.99 % purity) and pure aluminum (99.99 % purity) and provided satisfactory agreement with literature values.

2.1 Central Specimen Stack

A schematic cross-section view of the NPL axial heat flow apparatus is shown in Fig. 1. This apparatus creates a temperature gradient along a cylindrical rod specimen (20 mm in diameter and 160 mm long) that is screwed onto a water-cooled base at the bottom and has a guarded specimen heater unit firmly clamped to its upper flat surface using a spring and screw arrangement at the top. To ensure good thermal contact at each end of the specimen, both ends of the specimen are machined flat to better than 0.02 mm and the upper surface sprayed with a thin layer of graphite paint. The temperature gradient along the specimen is measured using seven N-type bare-wire thermocouples

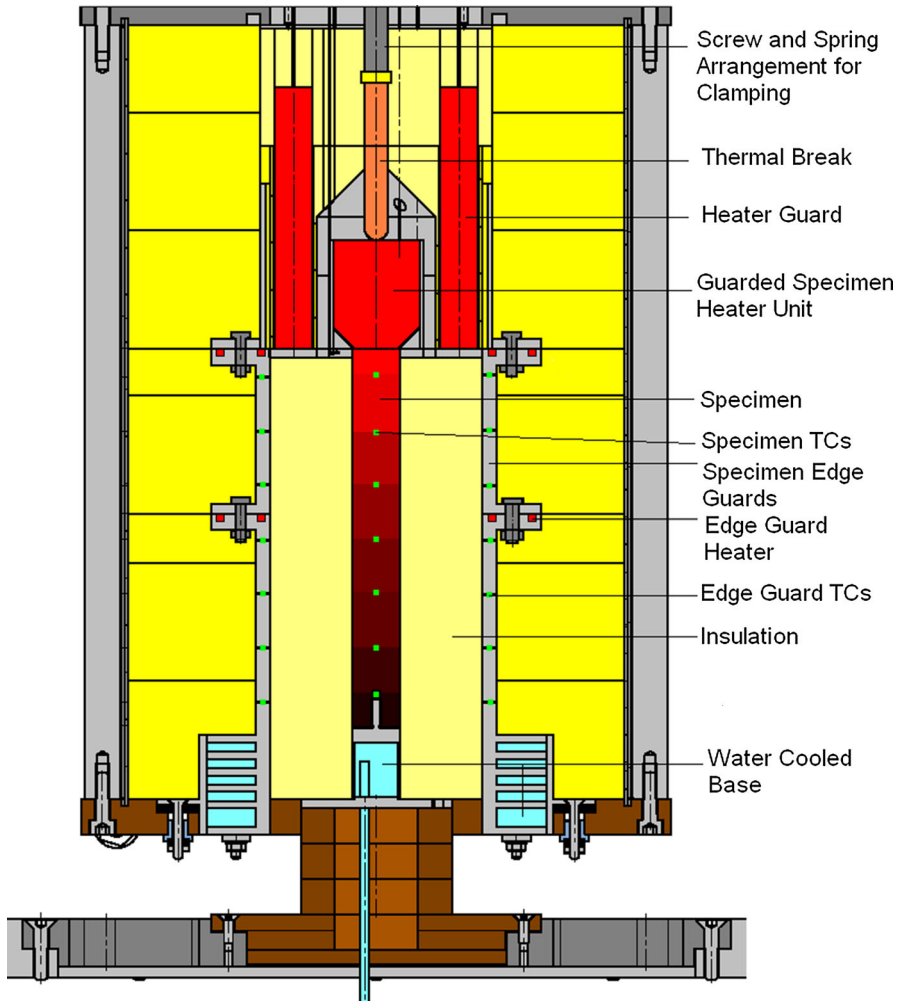


Fig. 1 Schematic diagram of the NPL axial heat flow apparatus

(0.2 mm diameter) inserted into evenly distributed holes drilled in the specimen, with each hole having a diameter of 0.55 mm and a depth of 5 mm. To minimize heat loss along the thermocouples, they are kept in an isothermal region for as long as practical. Each thermocouple is protected with high-temperature insulation sleeves and then wrapped horizontally around the specimen before they pass out from the edge-guard enclosure.

The uppermost thermocouple is located 10 mm below the top specimen surface to allow the effect of any temperature non-uniformities at the top interface to diminish. The remaining six thermocouples are located at 23 mm intervals along the length of the specimen and thereby divide the specimen into six individual measurement zones.

2.2 Specimen Heater Assemblies

The heat applied to the upper surface of the specimen is supplied by a specimen heater that consists of a compact metal-sheathed cartridge heater (60 V, 150 W) supplied by Watlow Ltd., which is inserted horizontally into a cylindrical block of nickel alloy 201 with a diameter of 40 mm and its end tapered down to 20 mm diameter to match the specimen diameter in the primary configuration. The upper temperature and thermal-conductivity limits of the apparatus are constrained by the maximum service temperature and power of the compact specimen heater. The specimen heater is surrounded radially and above by a thin layer of high-density fibrous insulation and then by a cylindrical heated guard which is also made from nickel alloy 201 and has a wall thickness of 20 mm. There are six cartridge heaters mounted vertically in the heated guard and controlled by digital controllers responding to the outputs of a differential thermocouple (N-type) embedded in the specimen heater unit and the heated guard. This allows the heated guard surrounding the specimen heater to be controlled to the same temperature as the specimen heater, which ensures that the heat generated in the specimen heater flows axially downwards through the specimen. To achieve good thermal contact between the specimen heater and the specimen, a clamping screw is used to apply compressive load through a mullite ceramic tube that passes through a small hole in the upper part of the heated guard. The mullite ceramic tube is filled with high density fibrous insulation and acts as a thermal break to minimize the heat passing through to a negligible amount.

2.3 Edge-Guard System

To ensure the heat generated in the specimen heater unit is constrained to flow axially downwards through the specimen with minimum lateral loss or gain of heat, the specimen is surrounded by an actively controlled linear edge-guard system. Directly wrapped around the specimen is a thin layer of high density fibrous insulation that fills in any gaps around thermocouples, and then surrounding this is another layer of insulation that has a thickness of about 30 mm. The insulation is surrounded by a stainless-steel edge-guard system that is formed by a pair of half cylinders (internal diameter of 90 mm and wall thickness of 6 mm) that are mounted on hinges and are closed around the specimen and insulation during the measurements. Each half of the edge-guard has two independently controlled cable heaters at different heights and is water-cooled at the bottom level. There are seven mineral-insulated metal-sheathed N-type thermocouples (1 mm outer diameter) embedded in each half of the edge-guard and aligned at same height levels as those in the specimen. The power to the heaters on the edge-guard can be adjusted to achieve a match between the temperature measurements on the edge-guard and the corresponding measurements in the specimen. The flow of cooling water in the base of the edge guard (as shown in Fig. 1) can also be adjusted to give a closer match, and air can be used instead of water for specimens with a thermal conductivity above $40 \text{ W}\cdot\text{m}^{-1}\cdot\text{K}^{-1}$. The edge-guard system is surrounded by a thick layer of micro-porous insulation to reduce heat loss to the laboratory environment. For specimens with a thermal conductivity below $40 \text{ W}\cdot\text{m}^{-1}\cdot\text{K}^{-1}$,

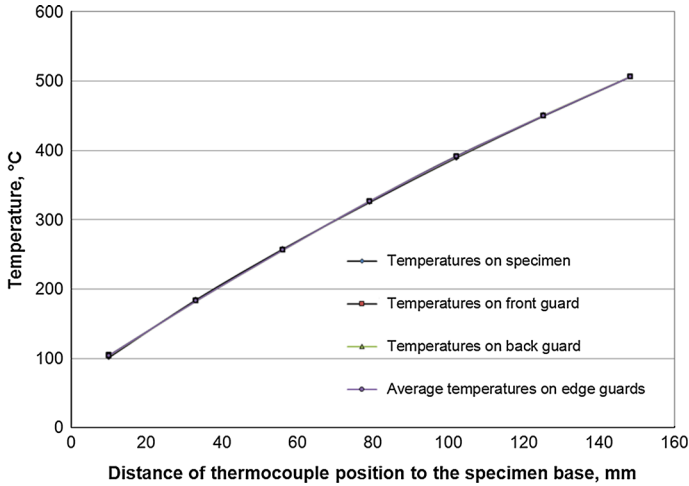


Fig. 2 Temperature profiles on the specimen and edge guards

the temperature agreement between the edge guard and the edge of the specimen at the same height is normally within 3 K. For specimens with a thermal conductivity greater than $40 \text{ W} \cdot \text{m}^{-1} \cdot \text{K}^{-1}$, the temperature agreement is within 5 K.

A typical temperature profile on the edge-guard and specimen during thermal-conductivity measurements in the NPL axial heat flow apparatus is shown in Figs. 2 and 3. The specimen in these examples was made from the thermal-conductivity reference material NPL 2S89 (based on Stainless Steel 310). In Fig. 2, the diamond symbols represent the temperatures of the specimen measured at seven positions relative to the base of the specimen. The square and triangle symbols represent the temperatures on the front half of the edge-guard and the back half of the edge-guard, respectively. The filled circles represent the average temperatures on the edge-guard. A closer look at the temperature mismatches shown in Fig. 3 reveals that the temperature difference between the front and back guards (diamond symbols) is within $\pm 1 \text{ K}$ in all six zones. The average temperature of the edge-guard matches with those on the specimen to within $\pm 3 \text{ K}$ (square symbols) in all six zones. The error bar on each point indicates the calibration uncertainty of each thermocouple, which was $0.5 \text{ }^\circ\text{C}$ for temperatures below $500 \text{ }^\circ\text{C}$ and $0.6 \text{ }^\circ\text{C}$ at $500 \text{ }^\circ\text{C}$.

2.4 Summary of Measurement Procedure

Once the system has reached an initial equilibrium under the control of temperature controllers for each of the heaters, a constant power is set on the specimen heater using a high-stability linear power supply (direct current). The magnitude of this constant power is determined by monitoring the average power that was supplied while under the temperature control. An accurate value of the constant power to the specimen heater is calculated from measurements of the voltage drop directly across the cartridge heater connections within the specimen heater and from the voltage drop across a

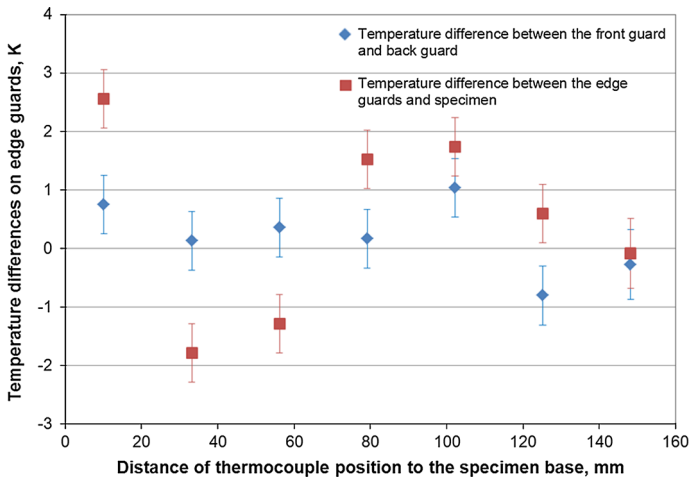


Fig. 3 Temperature difference between the front guard and back guard, and between the edge guard and specimen

calibrated standard resistor connected in series with the cartridge heater. These voltages and all thermocouple outputs are logged automatically during the approach to equilibrium and during the thermal-conductivity measurement by means of a computer-controlled switching system incorporating a digital voltmeter with a resolution of $0.1 \mu\text{V}$.

A set of equilibrium criteria is used to determine when the test system has reached sufficient steady-state heat transfer conditions to provide the required accuracy. These criteria include: temperature matches between the heated guard and specimen heater; temperature matches between the edge-guard temperatures and specimen temperatures; the stability of the calculated thermal-conductivity value; and the stability of the temperature difference across each of the six measurement zones along the specimen. The temperature of the heated guard is adjusted to match that of the specimen heater to within 0.1 K. The temperature of the front and back halves of the edge-guard is adjusted separately and matched within better than 1.5 K at each zone. For specimens with a thermal conductivity less than $40 \text{ W}\cdot\text{m}^{-1}\cdot\text{K}^{-1}$, the temperature difference between the edge-guard and the specimen at each zone is adjusted to be within 3 K. For specimens with a thermal conductivity greater than $40 \text{ W}\cdot\text{m}^{-1}\cdot\text{K}^{-1}$, the temperature difference between the edge-guard and the specimen at each zone is adjusted to be within 5 K. These limits of temperature mismatch ensure that heat loss or gain from the specimen edge normally contributes less than 1% of the axial heat flow rate through the specimen. Once these matching conditions have been satisfied, the system is monitored at regular intervals until the direction of drift in the calculated thermal-conductivity value is random and is less than $0.05 \text{ W}\cdot\text{m}^{-1}\cdot\text{K}^{-1}$. The drift in temperature difference of each zone of the specimen is also required to be random and less than 0.1 K. Once all these criteria are reached, the final measurement data are recorded and reported for each of the six zones in terms of a measured thermal-conductivity value at a mean specimen temperature.

3 Assessment of Measurement Uncertainty

The assessment of the overall measurement uncertainty relating to measured thermal-conductivity values produced by the new NPL axial heat flow apparatus is based on differentiation of Eq. 1. It includes contributions from the uncertainty in measuring each of: the separation distance between thermocouple holes in the specimen that define the boundary of each of the six zones, Δx ; the cross-sectional area of the specimen in each zone, A ; the temperature difference across each zone, ΔT ; and the heating power applied to the specimen, Q , which includes the measurements of applied voltage, current, and heat losses or gains from the specimen heater and the edge of the specimen. The uncertainty in the mean temperature of a zone indirectly contributes to the overall uncertainty and is dependent on how significantly the test material's thermal conductivity varies with temperature. Long-term repeatability, reproducibility and stability of temperatures, and rate of heat flux density are also considered in calculating the overall measurement uncertainty for each thermal-conductivity value.

The contribution to the overall measurement uncertainty due to heat loss or gain from the specimen heater is determined experimentally by running the apparatus with the heated guard temperature intentionally offset by different amounts (up to 10 K) from the specimen heater temperature and monitoring the effect of this on the calculated thermal-conductivity value. The heat loss or gain due to the temperature mismatch between the specimen edge-guard and specimen was also investigated during initial performance checks by applying intentional temperature off-sets and it was normally found to contribute less than 1 % to the overall measurement uncertainty. However, due to practical constraints, for normal tests this contribution to the uncertainty is calculated based on: a thermal-conductivity value for the high density fibrous insulation wrapped around the specimen; the thickness of this insulation; and the temperature mismatches between corresponding thermocouples in the edge-guard and specimen for each temperature zone. For a particular temperature zone, this uncertainty due to heat loss or gain is calculated including the cumulative effect of the uncertainties in the higher temperature zones above.

By combining the individual uncertainties for each parameter being measured, the best overall measurement uncertainty for measured thermal-conductivity values is estimated to be within 3 %, based on a standard uncertainty multiplied by a coverage factor $k = 2$, providing a level of confidence of approximately 95 %. However, the overall estimated uncertainty for each specimen will vary depending on its material properties, the mean zone temperature, and other measured parameters. An individual uncertainty can be estimated and quoted for each measured value of thermal conductivity at the mean specimen temperature of a particular one of the six zones, or the maximum value for the entire specimen can be provided.

4 Proven Performance Checks Against Reference Materials

The measurement transducers in the NPL axial heat flow apparatus were calibrated with traceability to the United Kingdom's primary national standards and a wide range of performance checks carried out, including: offsetting the temperatures of

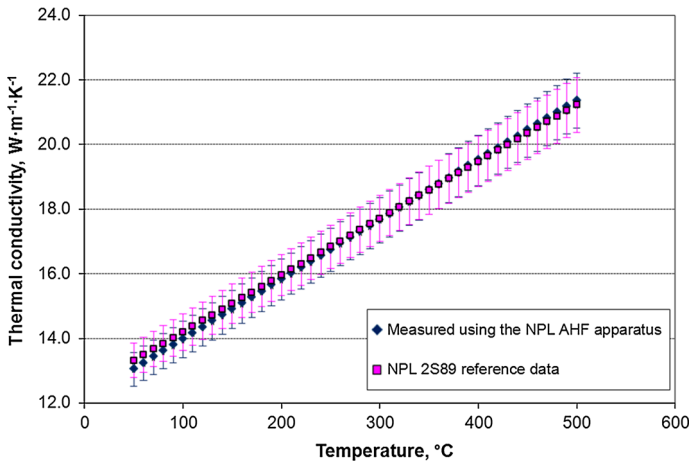


Fig. 4 Proven performance check of the NPL AHF apparatus against the existing NPL reference material 2S89

guarding systems; extended stability monitoring beyond the point of equilibrium; reproducibility and repeatability tests; and production of a detail uncertainty budget. The NPL axial heat flow apparatus was then validated up to $80 \text{ W} \cdot \text{m}^{-1} \cdot \text{K}^{-1}$ against certified reference materials NPL 2S89 and BSC Pure Iron.

In Fig. 4, a comparison is shown between the measured thermal-conductivity values using the NPL axial heat flow apparatus on a specimen made from certified reference material NPL 2S89 and the published data [6]. The diamond symbols represent the measured thermal-conductivity values using the NPL axial heat flow apparatus, and the bar on each point indicates its estimated measurement uncertainty of 4.0 % with a 95 % confidence limit. The square symbols represent the reference values of the NPL 2S89 and the bar on each point indicates the quoted uncertainty for this reference material of 4.0 % with a 95 % confidence limit. The agreement between the two sets of data is within 2 % over the entire temperature range of the NPL axial heat flow apparatus.

Figure 5 shows a comparison between the measured thermal-conductivity values using the NPL axial heat flow apparatus and previous NPL reference data on a specimen made from BSC Pure Iron [8], which was measured using the NPL standard the Long-Bar apparatus. The diamond symbols represent the measured thermal conductivities using the NPL axial heat flow apparatus, and the bar on each point indicates its estimated measurement uncertainty of 5.5 % with a 95 % confidence limit. The square symbols represent the NPL reference values for the BSC Pure Iron material and the bar on each point is its uncertainty of 4.0 % at a 95 % confidence limit. The agreement between the two sets of data is within 3 % over the entire temperature range of the NPL axial heat flow apparatus.

5 Conclusions

NPL has designed a new axial heat flow apparatus to help meet increasing demand from industry and academia for accurate thermal properties values for high thermal-

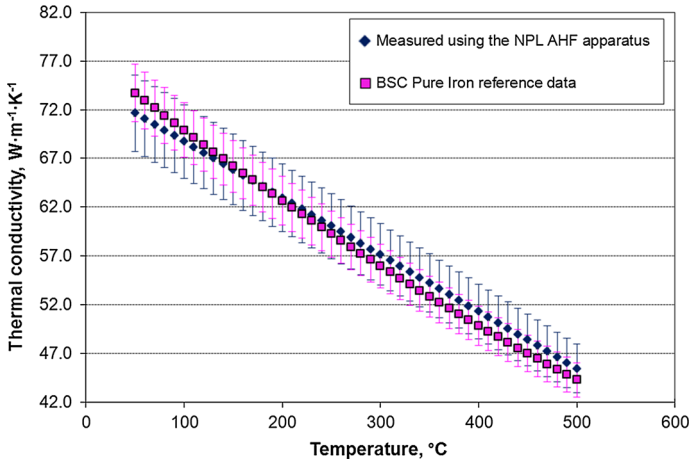


Fig. 5 Proven performance check of the NPL AHF apparatus against the existing NPL reference material BSC Pure Iron

conductivity materials. The new facility can provide measurements of thermal conductivity on industrial materials from $10 \text{ W}\cdot\text{m}^{-1}\cdot\text{K}^{-1}$ to $240 \text{ W}\cdot\text{m}^{-1}\cdot\text{K}^{-1}$ at temperatures from $50 \text{ }^\circ\text{C}$ to $500 \text{ }^\circ\text{C}$ and also be used to produce a new range of reference materials to calibrate industrial measurement techniques. The main improvement over the previous NPL apparatus is the level of temperature matching between the edge-guard system and the edge of the specimen, which helps to ensure that heat applied to the specimen is constrained to flow axially downwards through the specimen with minimum radial loss or gain of heat. The temperature profiles shown in Figs. 2 and 3 reveal that during thermal-conductivity measurements, the temperature difference between the front and back of the new guarding system is typically within $\pm 1 \text{ K}$ and the average temperatures on the edge-guard matches with those on the specimen within $\pm 3 \text{ K}$.

The apparatus has been validated for thermal conductivities below $80 \text{ W}\cdot\text{m}^{-1}\cdot\text{K}^{-1}$ against the existing NPL thermal-conductivity reference materials NPL 2S89 and BSC Pure Iron. It has also been satisfactorily tested on higher thermal conductivities up to $240 \text{ W}\cdot\text{m}^{-1}\cdot\text{K}^{-1}$ using pure zinc and aluminum with a narrow specimen configuration to increase the thermal resistance of the test specimen. The agreement between measurements in the NPL axial heat flow apparatus and published reference data for temperatures from $50 \text{ }^\circ\text{C}$ to $500 \text{ }^\circ\text{C}$ was within 2 % for NPL 2S89 and within 3 % for BSC Pure Iron. The uncertainty in measurements using the axial heat flow apparatus on a specimen of NPL 2S89 is estimated to be within 4.0 % and on a specimen of BSC Pure Iron is estimated to be within 5.5 %. These estimations are based on a standard uncertainty multiplied by a coverage factor $k = 2$, providing a level of confidence of approximately 95 %.

6 Future Plans

The newly designed and validated NPL axial heat flow apparatus is now a UK National Standard. It has been used for characterizing new stocks of thermal-conductivity

references in compliance with ISO Guide 34. The new stocks of thermal-conductivity reference materials are based on materials Stainless Steel 304, Inconel 600 and pure iron. A paper on the development of new thermal-conductivity reference materials is being prepared for submission.

Acknowledgment This work was funded by the National Measurement Office of the United Kingdom.

References

1. C. Jensen, C. Xing, C. Folsom, H. Ban, J. Phillips, *Int. J. Thermophys.* **33**, 311 (2012)
2. R.L. Kallaher, C.A. Latham, F. Sharifi, *Rev. Sci. Instrum.* **84**, 013907 (2013)
3. ASTM E1225-04, *Standard Test Method for Thermal Conductivity of Solids by Means of the Guarded-Comparative-Longitudinal Heat Flow Technique* (ASTM International, West Conshohocken, PA, 2004)
4. ASTM E1461-01, *Standard Test Method for Thermal Diffusivity by the Flash Method* (ASTM International, West Conshohocken, PA, 2001)
5. W.J. Parker, R.J. Jenkins, C.P. Butler, G.L. Abbott, *J. Appl. Phys.* **32**, 1679 (1961)
6. J. Clark, R. Tye, *High Temp. High Press.* **35/36**, 1 (2003/2004)
7. J.M. Corsan, in *Compendium of Thermophysical Property Measurement Methods*, vol. 2, ed. by K.D. Maglic, A. Cezairliyan, V.E. Peletsky (Plenum Press, New York, 1992), pp. 3–31
8. J. Clark, A. Kibble, J. Redgrove, “Report on Thermophysical Property Data on Key Engineering Materials,” NPL Report CBTLM S44, available upon request at the web site www.npl.co.uk (National Physical Laboratory, Teddington, UK), p. 27
9. D.R. Flynn, H.E. Robinson, in *Proceedings of the Thirtieth International Thermal Conductivity Conference*, ed. by D.S. Gaal, P.S. Gaal (DEStech Publications Inc., Lancaster, PA, 2010), pp. 542–551